

Engine Re-start Transient Simulation Tool for Cryogenic Liquid Rocket System

*Yu Daimon**, *Yutaka Umemura***, *Yoshio Nunome****, and *Tetsufumi Ohmaru, Masao Toyama, Takenori Nakajima†*

**Japan Aerospace Exploration Agency (JAXA)*

Tsukuba, Ibaraki, 305-8505, Japan, daimon.yu@jaxa.jp

***Japan Aerospace Exploration Agency (JAXA)*

Tsukuba, Ibaraki, 305-8505, Japan, umemura.yutaka@jaxa.jp

****Japan Aerospace Exploration Agency (JAXA)*

Kakuda, Miyagi, 981-1525, Japan, nunome.yoshio@jaxa.jp

†Ryoyu Systems Co., Ltd.

Minota-ku, Tokyo, 108-0074, Japan

Abstract

The aim of this study is to develop a combustion chamber component model for predicting combustion chamber pressure transient for a system analysis. To understand and evaluate the mass flow rate of LOX and GH₂ for the combustion chamber component model, single element firing tests are conducted. A phase change state of LOX through a LOX manifold and orifice is revealed from measured data in a LOX manifold and combustion chamber. The mass and energy conservation equations for appropriate phase change state, which is observed in the experimental data, are utilized in the combustion chamber component model.

1. Introduction

Future space transport systems aim at breaking the cost barrier with reusable liquid rockets for both the 1st and 2nd stages [1, 2]. Recently, there has been much interest in developing a reusable launch vehicle with refueling from an in-orbit propellant depot, focusing largely on transporting payloads to Mars. With the number of flights on the increase, simulations of reusable liquid rockets will be used to predict the performance of transient operations such as engine start-up and shut-down, and to reduce the amount of propellant used during transient operation.

JAXA is developing an operation evaluation tool to aim for high specific thrust of reusable cryogenic liquid rockets. The first objective of this tool is used to simulate the reignition operation of the reusable rocket accurately, with the aim of reducing the amount of propellant used. There are three steps to reignition: precooling the turbo pump, starting combustion by pressure in the propellant supply tank (idle mode combustion), and initiating next combustion when the turbo pump starts up. To evaluate turbo pump precooling and the idle mode combustion, it is necessary to understand the dynamic responses for fluid and heat transfer. Computational Fluid Dynamics (CFD) is usually an effective method of analysis, but the computational costs are too high and CFD is poorly suited to doing operational analysis. Therefore, we have conceived a system-level simulation that can evaluate the transient sequence of engine reignition (for example, one-dimensional thermal flow analysis using the node-link network approach). Results of CFD analysis help to understand key phenomena and to build a simple component model for system-level simulation.

In this paper, the combustion chamber component model is developed for prediction of the combustion chamber pressure transient during idle mode combustion. The combustion pressure transient is determined by the mass flow rate of the propellant sent to the combustion chamber. It is difficult to predict the mass flow rate during start-up because the pressure loss in the flow path to the combustion chamber varies. Therefore, the thermal fluid in the flow path was clarified by single element firing tests conducted at the Kakuda Space Center of JAXA, and the combustion chamber component model predicted variable mass flow rates and combustion chamber pressure.

2. Experimental apparatus

Figure 1a shows the combustion chamber developed for this study. It consists of an injector, a visualization window, a cylinder, and a nozzle part. The inner diameter of the cylinder part is 30 mm. The nozzle diameter is 16 and 12.75 mm for low and high combustion pressure cases, respectively. The distance from the face plate to the nozzle throat is 219 mm. The size of the visualization window is 23mm x 16mm. On the visualization window, the film cooling gas was injected to protect a brake of the window. Figure 1b is a close-up view of the injector part showing the positions of the pressure and temperature sensors. The liquid oxygen (LOX) manifold has pressure (POI) and temperature (TOI) sensor ports. The gaseous hydrogen (GH₂) manifold has pressure (PFI) and temperature (TFI) sensor ports. The combustion pressure (PC) was measured near the face plate.

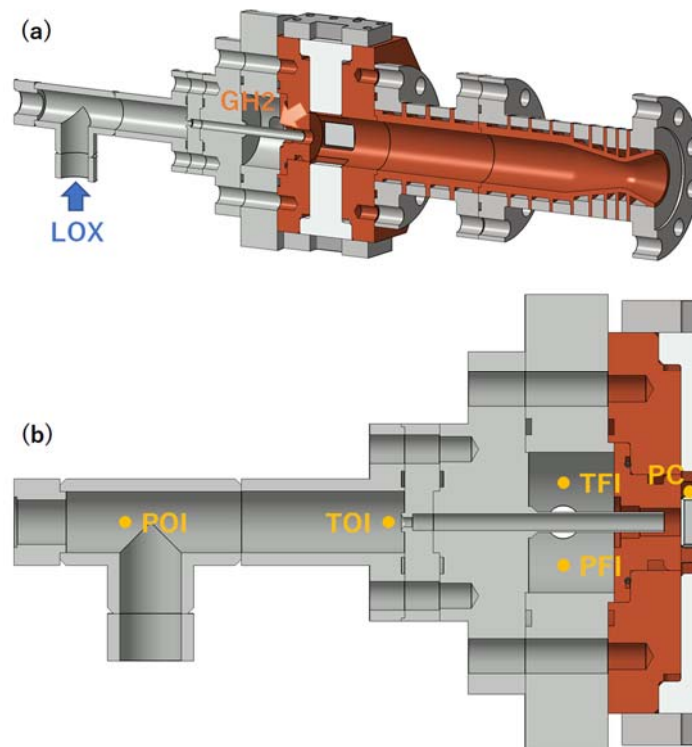


Figure 1: Schematic of the combustion test apparatus

Figure 2 shows valve sequences. LOX and GH₂ lines have sub-valves and main-valves, respectively. The torch igniter at the nozzle exit was ignited at least 1 sec before the LOX sub-valve was opened ($t = 11.1$ sec). Subsequently, the GH₂ sub-valve was opened at $t = 11.2$ sec. The main-valves for LOX and GH₂ were opened at $t = 11.9$ and 12.05 sec, respectively. And the sub-valves of LOX and GH₂ were closed at $t = 12.2$ and 12.4 sec, respectively, after the main-valves opened.

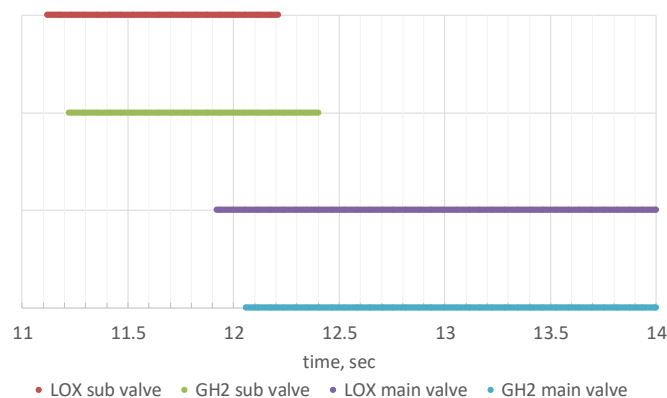


Figure 2: Valve sequences

Table 1 shows the experimental conditions. The main parameters were the combustion pressure and whether the LOX manifold was pre-cooled. The low and high combustion pressures correspond to subcritical and supercritical conditions for LOX, respectively. In Cases 1 and 3, the LOX manifold was cooled by LOX just before the combustion test. In Cases 2 and 4, the LOX manifold was not pre-cooled.

Table 1: Experimental conditions

	Combustion Pressure (PC)	O/F total	O/F core	Pre-cooling
Case 1	2.87	6.93	9.72	yes
Case 2	2.91	5.93	7.83	no
Case 3	6.95	3.32	4.96	yes
Case 4	6.97	3.18	4.96	no

3. Results and discussion

3.1 Correlation of the time history of thermodynamic state and the valve sequences

Before details are discussed, the correlation between the measured time histories of the thermodynamic state and the valve sequences will be explained using a typical time history. Figure 3 shows the combustion pressure history (PC), LOX manifold pressure (POI) and temperature (TOI) histories upstream of the LOX orifice, and GH₂ manifold pressure (PFI) and temperature (TFI) in Case 1. The LOX sub-valve was opened at $t = 11.1$ sec. POI and TOI sensors showed a rise at $t = 11.35$ sec when the LOX reaches the manifold upstream at the LOX orifice. The GH₂ sub-valve was opened at $t = 11.2$ sec. PFI and TFI sensors showed a rise at $t = 11.6$ sec. Oxygen and hydrogen reach the combustion chamber at almost the same time that the mixture ignited by the torch igniter at the nozzle exit. Ignition in the combustion chamber was observed as PC rise just after PFI rise at $t = 11.65$ sec. The main-valves for LOX and GH₂ were opened at $t = 11.9$ and 12.05 sec respectively. The mass flow rate increases as the POI and PFI rises steeply at $t = 12.2$ and 12.3 sec respectively. PC showed a steep pressure rise just after PFI rise at $t = 12.3$ sec. After $t = 12.6$ sec, the pressure reaches an almost steady state. TFI is almost constant, around 280 K. On the other hand, TOI changes from 200 to 110 K. The combustion pressure depends on the density of LOX (i.e., its phase). Following this section, the LOX phase will be discussed for the subcritical and supercritical cases.

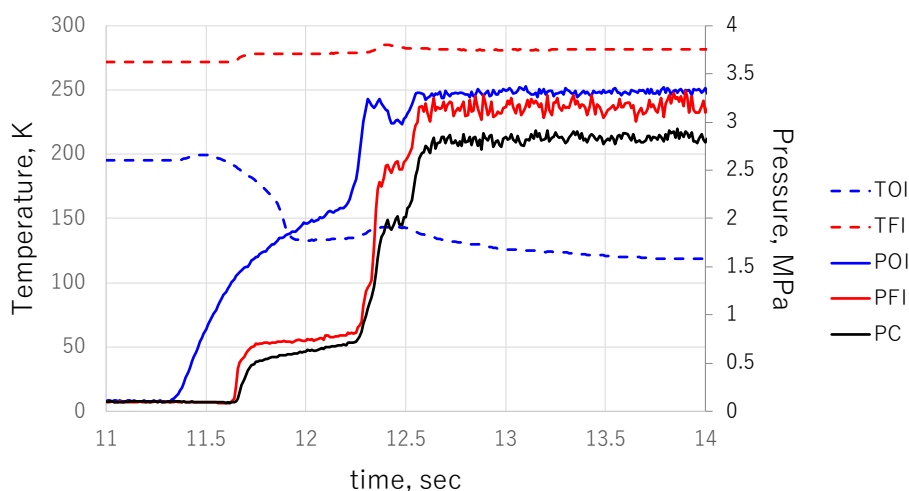


Figure 3: Measured pressures and temperatures

3.2 Subcritical conditions

This section describes the relation between the phase change of LOX and the combustion pressure history by comparing LOX fluid in the manifold against saturation properties. Figure 4 shows the combustion pressure history (PC), LOX manifold pressure (POI), and temperature (TOI) histories upstream of the LOX orifice for Case 1. In addition, the figure also includes the saturation pressure (PSAT) and temperature (TSAT) history upstream of the LOX orifice. Before $t = 12.25$ sec, the time history of the thermodynamic state shows $POI < PSAT$ and $TOI > TSAT$. These indicate that LOX has become gaseous oxygen. LOX vaporizes in the manifold due to heat conduction from the manifold wall because the mass flow rate through the sub-valve is small. After the main-valve was opened, POI was larger than PSAT from $t = 12.25$ sec to $t = 12.4$ sec. This relation indicates that the LOX has reached the manifold upstream of the LOX orifice. In contrast, the differential pressure $POI - PC$ for $t = 12.25 - 12.4$ sec was almost equal to that before $t = 12.25$ sec. This suggests that LOX evaporated at the LOX orifice. For $t = 12.4 - 12.57$ sec, POI was smaller than PSAT and the differential temperature $TOI - TSAT$ was very small. These indicate that LOX became a two-phase flow. After $t = 12.57$ sec, the time history shows $POI > PSAT$ and $TOI < TSAT$, indicating LOX has reached the LOX manifold. The differential pressure ($POI - PC$) of LOX after $t = 12.57$ sec was smaller than that before $t = 12.25$ sec which indicates the presence of gaseous oxygen. This discussion describes that the thermodynamic state in the LOX manifold dominated the differential pressure. Furthermore, the thermodynamic state in the LOX orifice decided the mass flow rate.

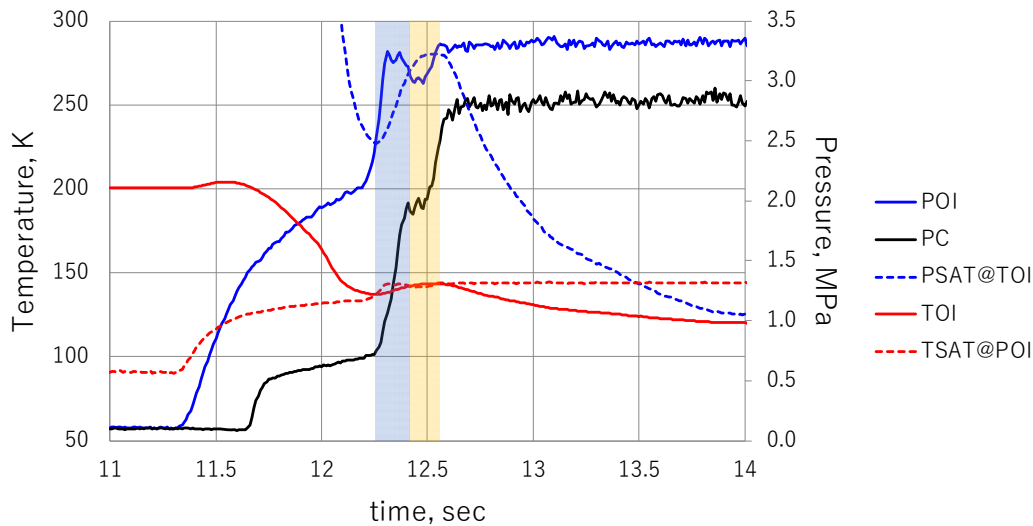


Figure 4: Time histories of measured and saturation properties

To understand the phase change of oxygen at the LOX orifice more clearly, the relation between the differential pressure ($POI - PC$) and the manifold pressure (POI) will be investigated. Figure 5 shows the relation between $POI - PC$ and POI. The time between $t = 11.7$ and 12.19 sec corresponds to the pressure rise after the sub-valve opened. Subsequently, the time between $t = 12.19$ and 12.31 sec corresponds to the pressure rise after the main-valve opened. The slope between $t = 11.7$ and 12.31 sec was almost constant. This tendency indicated that density was almost constant, in other words, gaseous oxygen exited through the LOX orifice. As shown in Fig. 4, the thermodynamic state in the LOX manifold upstream of the orifice indicated a liquid phase between $t = 12.25 - 12.4$. However, Fig. 5 indicates that the thermodynamic state at the LOX orifice was gaseous oxygen until $t = 12.31$ sec. Obviously, LOX evaporated at the orifice between $t = 12.25$ and 12.31 sec. Between $t = 12.31$ and 12.57 sec, the slope is not stable as shown in Fig. 5. This time slot corresponds to the two-phase flow between $t = 12.4 - 12.57$ as shown in Fig. 4. After $t = 12.57$, the differential pressure is low and almost constant (Fig. 5). This is typical characteristic of the liquid phase. As mentioned above, the differential pressure indicates the phase state of LOX in the orifice.

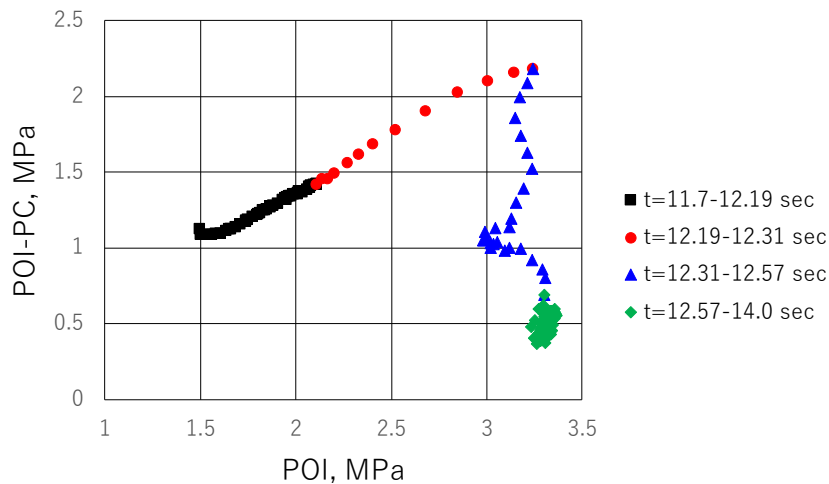


Figure 5: Relation between the differential pressure, POI – PC, and the manifold pressure, POI

The combustion pressure steep rise was induced by the liquid phase of oxygen as shown in Fig. 4. In the next case, the static firing test of the single element was performed without pre-cooling the LOX manifold. As shown in Fig. 4, Fig. 6 shows PC, POI, TOI, PSAT, and TSAT for the LOX manifold in Case 2. TOI was 288 K at $t = 11.5$ sec after the sub-valve opened. This high-temperature oxygen is the result of there being no pre-cooling. The pressure variations due to the LOX sub-valve opening, the GH_2 sub-valve opening, and the ignition occurring in combustion chamber were similar to those in Fig. 4. In contrast, the relation between POI and PSAT after the LOX main-valve opened was different from Fig. 4 with pre-cooling. POI was dramatically increased at $t = 12.23$ sec by the opening of the LOX main-valve. Unlike the pre-cooling case of Fig. 4, PSAT was much larger than POI after the LOX main-valve opened. Until $t = 12.9$ sec, oxygen in the LOX manifold was a gas. The characteristic of two-phase flow at the LOX orifice was observed at the same time. The differential pressure (POI – PC) became small between $t = 12.5$ and 12.9 sec. In addition, the differential temperature (TOI – TSAT) became very small between $t = 12.74$ and 12.98 sec. After $t = 12.9$ sec, POI was larger than PSAT. This indicates that LOX reached the manifold.

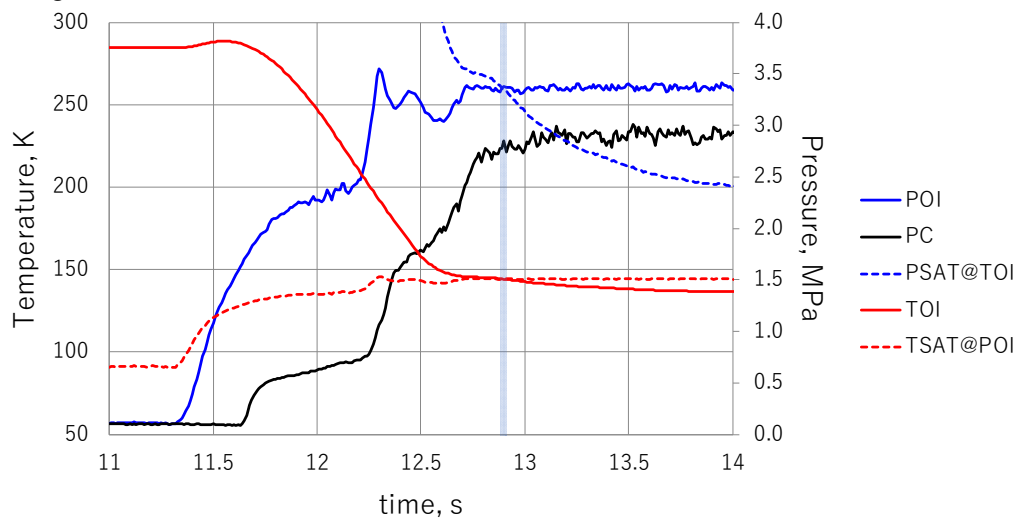


Figure 6: Time histories of measured and saturation properties

Figure 7 shows the relation between POI – PC and POI for Case 2. The time from $t = 11.7$ to 12.2 sec corresponds to the pressure rise after the sub-valve opened. Subsequently, the time between $t = 12.2$ and 12.3 sec corresponds to the pressure rise after the main-valve opened. The slope between $t = 11.7$ and 12.3 sec was almost constant. Both this and POI vs PSAT in Fig. 6 indicate that the gaseous oxygen has reached the LOX orifice. Between $t = 12.3$ and 12.9 sec, the slope was not stable. This indicates a two-phase flow at the orifice between 12.3 and 12.9 sec, although oxygen in the LOX manifold had become a gas before $t = 12.9$ sec in Fig. 6. Finally, POI – PC became constant after $t = 12.9$ sec. This timing shows that LOX reached the manifold as shown in Fig. 6.

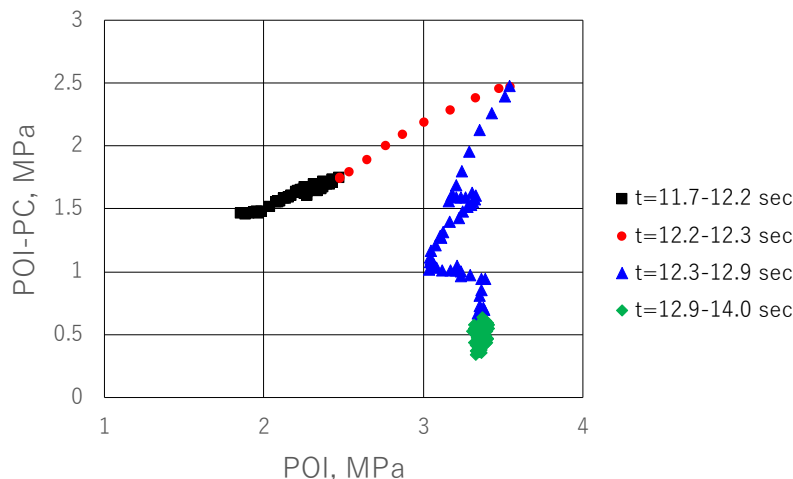


Figure 7: Relation between the differential pressure, POI – PC, and the manifold pressure, POI

3.3 Supercritical conditions

Figure 8 shows the combustion pressure history (PC), LOX manifold pressure (POI), and temperature (TOI) histories upstream of the LOX orifice in Case 3, which corresponds to a typical supercritical condition. This figure also includes the saturation pressure (PSAT) and temperature (TSAT) history upstream of the LOX orifice. The pressure variations due to the LOX sub-valve opening, the GH2 sub-valve opening, and the ignition occurring in the combustion chamber were similar to those of Fig. 4. At $t = 12.17$ sec, POI increased dramatically and as a result, TSAT also increased. Two-phase flow, characterized by a very small differential temperature (TOI – TSAT) over a period in the subcritical cases, did not appear. After $t = 12.37$ sec, the differential pressure was almost constant. In addition, POI was larger than PSAT, and TOI was smaller than TSAT. These are characteristics of the liquid phase. However, the pressure was greater than the critical pressure of LOX. Therefore, LOX was a supercritical fluid at this point.

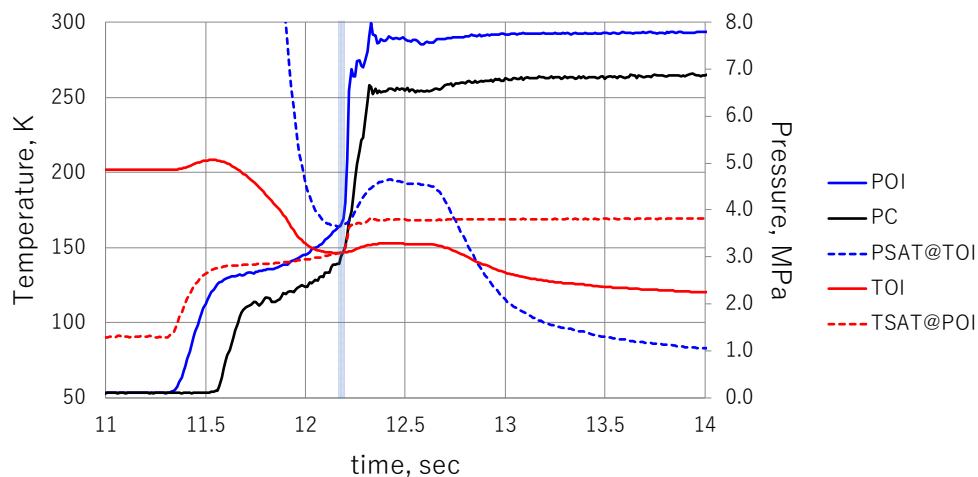


Figure 8: Time histories of measured and saturation properties

Figure 9 shows the relation between POI – PC and POI for Case 3. The time from $t = 11.8$ to 12.17 sec corresponds to the pressure rise after the sub-valve opened. Subsequently, the time between $t = 12.17$ and 12.23 sec corresponds to the pressure rise after the main-valve opened. This transition was similar to the other cases and corresponded to the characteristics of the gas flow through the LOX orifice. Between $t = 12.23$ and 12.37 sec, the differential pressure (POI – PC) became small. This seemed to correspond to a two-phase flow in the subcritical cases, but this is not strictly correct because POI is larger than the critical pressure of LOX. Although it is different from a phase change, it is likely that a large density change appeared due to the thermodynamic state crossing Widom line. This transient range was very short and a characteristic of the supercritical case. Finally, POI – PC was constant after $t = 12.37$ sec.

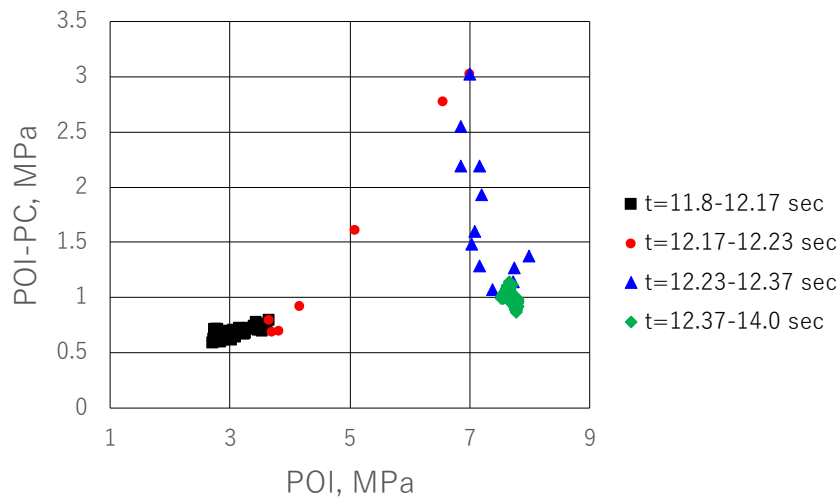


Figure 9: Relation between the differential pressure, POI – PC, and the manifold pressure, POI

In the same way as Fig. 8 shows, Fig. 10 shows PC, POI, TOI, PSAT, and TSAT for the LOX manifold in Case 4 which is the supercritical condition without pre-cooling of the LOX manifold. The pressure variations due to the LOX sub-valve opening, the GH_2 sub-valve opening, and the ignition occurring in the combustion chamber were all similar to those shown in Fig. 8. POI was dramatically increased at $t = 12.23$ sec by the opening of the LOX main-valve. Unlike Fig. 8 with pre-cooling, PSAT was larger than POI after the LOX main-valve opened. Between $t = 12.46$ and 12.67 sec, POI and PSAT intersected several times and the differential temperature, TOI – TSAT, is very small. This is similar to the subcritical case with pre-cooling (Case 1), which indicates a two-phase flow. However, the pressure level was over of the critical pressure of LOX, so the thermodynamic property seems to be related to a pseudo supercritical state. After $t = 12.67$ sec, POI was larger than PSAT and the differential pressure, POI – PCI, was almost constant.

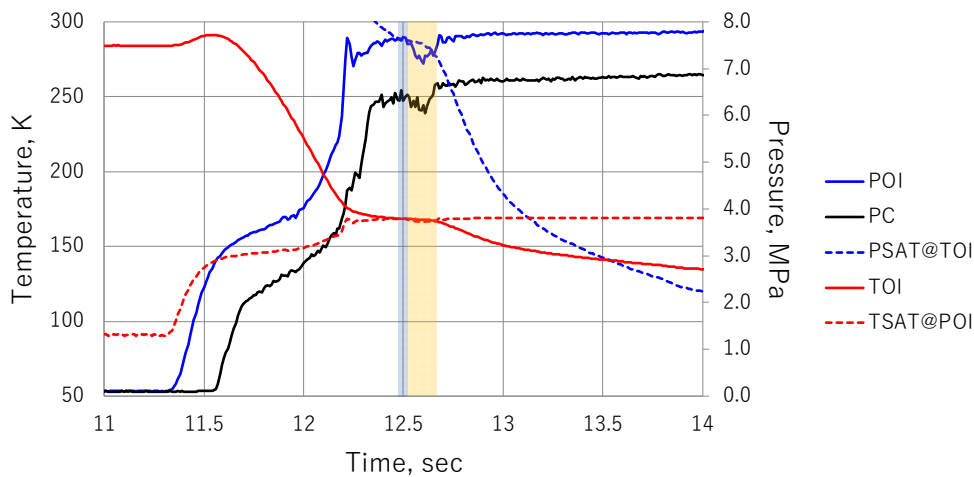


Figure 10: Time histories of measured and saturation properties

Figure 11 shows the relation between POI – PC and POI in Case 4 without pre-cooling the LOX manifold. The time between $t = 11.8$ and 12.1 sec corresponds to the pressure rise after the sub-valve opened. Subsequently, the time between $t = 12.1$ and 12.23 sec corresponds to the pressure rise after the main-valve opened. The slope between $t = 11.8$ and 12.23 sec is almost constant. This indicates that gaseous oxygen reached the LOX orifice. Between $t = 12.3$ and 12.9 sec, the differential pressure, POI – PC, decreased. This indicates a large density change due to the thermodynamic state crossing Widom line. Finally, POI – PC was constant after $t = 12.67$ sec. Except for the length of this transient time $t = 12.23 - 12.67$, the characteristics were similar to Case 3 with pre-cooling of the LOX manifold.

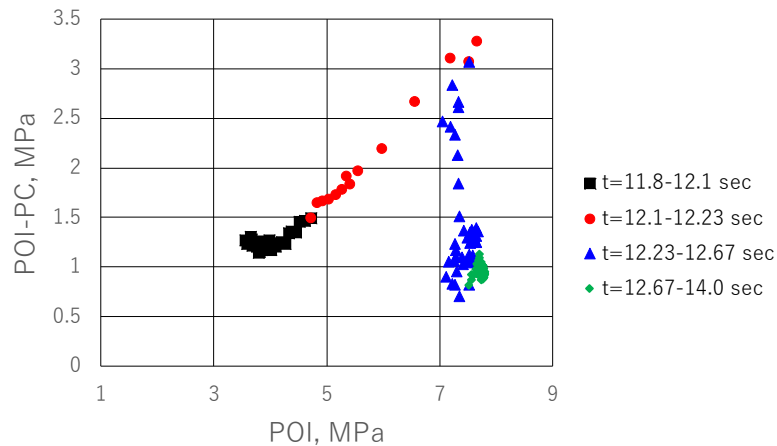


Figure 11: Relation between the differential pressure, POI – PC, and the manifold pressure, POI

3.4 Combustor modelling

As shown by the experimental data for the start-up transient, the thermodynamic state of oxygen in LOX manifold changed from gas to liquid. The combustion pressure was calculated by the mass flow rate, estimated by the differential pressure between the LOX manifold and the combustion pressure. This calculation was iterated for the mass flow rate and the combustion pressure using the mass and energy conservation equations. The input parameters were the pressure (POI) and temperature (TOI) of the LOX manifold. The output parameters were the combustion pressure and the mass flow rate. Figure 12 shows the combustion pressure for the experimental data (PC), the ideal gas theoretical equation (PC_ideal), and the incompressible liquid theoretical equation (PC_incomp) for Case 1. The results of the ideal gas equation reproduced the experimental data in $t = 11.6 - 12.35$ sec. Around $t = 12.35$ sec, POI was larger than PSAT as shown in Fig.4. The thermodynamic property of the LOX manifold indicated the liquid phase. However, it can be determined from Fig. 12 that the LOX became gaseous oxygen in the LOX orifice. After $t = 12.6$ sec, the results of the incompressible liquid equation reproduced the experimental data. Therefore, it suggested that two-phase flow occurred at the orifice between $t = 12.35 - 12.6$ sec. Future studies will develop combustion modelling for two-phase flow.

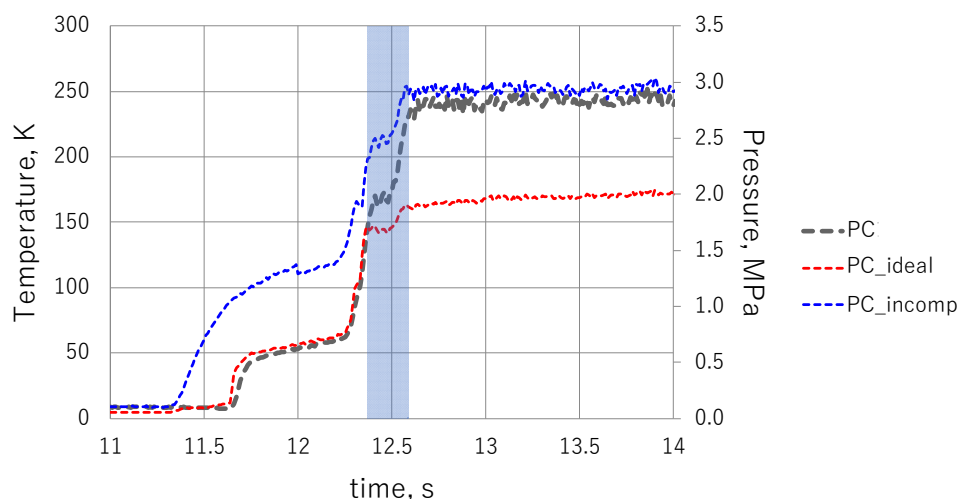


Figure 12: Time histories of measured and theoretical pressure

4. Conclusion

The single element firing tests were conducted at the Kakuda Space Center of JAXA to develop the combustion chamber component model for predicting the combustion chamber pressure transient for system analysis. The relation between the combustion pressure and the thermodynamic state in the LOX manifold were investigated. The thermodynamic state in the LOX manifold indicated that LOX became gaseous oxygen after the LOX sub-valve opened.

LOX vaporized in the manifold due to heat conduction from the manifold wall because the mass flow rate through the sub-valve was small. After the main-valve opened, the pre-cooling status of the LOX manifold dominated the thermodynamic state. With pre-cooling, the transient time from gas to liquid (including a supercritical state) was short. In contrast, the transient time for the cases with no pre-cooling was longer than that with pre-cooling. Based on these data, the combustion chamber component model for predicting the combustion chamber pressure transient was developed. The mass flow rate and the combustion pressure were calculated using the mass and energy conservation equations. The combustion pressure could be predicted by the theoretical prediction model except for the time range of the two-phase flow at the LOX orifice.

References

- [1] Glidden, G., L., and Wilhite, A., W., 2014. Performance of Existing Launch Vehicle Stages for Earth Departure with Refuel from Orbital Propellant Depot. In: *AIAA SPACE 2014 Conference and Exposition*. AIAA 2014-4272.
- [2] Tchou-Kien, D., 2017. PROMETHEUS, a low cost LOX/CH₄ Engine Prototype. In: *53rd AIAA/SAE/ASEE Joint Propulsion Conference*. AIAA 2017-4750.